Calculation of disconnected quark loops in lattice QCD*

Zhen Cheng(程贞)[1)] Jian-Bo Zhang(张剑波)[2)] Guang-Yi Xiong(熊光仪)[3)]

Department of Physics, Zhejiang University, Hangzhou 310027, China

Abstract: Calculation of disconnected quark loops in lattice QCD is very time consuming. Stochastic noise methods are generally used to estimate these loops. However, stochastic estimation gives large errors in the calculations of disconnected diagrams. We use the symmetric multi-probing source (SMP) method to estimate the disconnected quark loops, and compare the results with the $Z(2)$ noise method and the spin-color explicit (SCE) method on a quenched lattice QCD ensemble with lattice volume $12^3\times 24$ and lattice spacing $a\approx 0.1$ fm. The results show that the SMP method is very suitable for the calculation of pseudoscalar disconnected quark loops. However, the SMP and SCE methods do not have an obvious advantage over the $Z(2)$ noise method in the evaluation of the scalar disconnected loops.

Keywords: lattice QCD, Wilson matrix, disconnected quark loops, $Z(2)$ noise method, SMP method

DOI: 10.1088/1674-1137/44/3/033104

1 Introduction

Lattice QCD is a gauge invariant and nonperturbative regularization scheme for QCD that was introduced by K. Wilson in 1974 [1]. Many quantities can be obtained from the first principles by using a finite space-time lattice to simulate the interactions between quarks and gluons. The calculation of diagrams with disconnected quark loops is one of the most challenging problems in lattice QCD. Disconnected loops are needed in calculations of many lattice QCD observables, such as the nucleon electromagnetic form factors [2, 3], pi-NN coupling and pion polarizability [4], the mass of pseudoscalar flavor-singlet mesons [5, 6], strangeness and charm content of the nucleon [7, 8], hadronic scattering lengths and structure functions [9], and electron or muon hadronic $g-2$ loop contributions [10]. In the lattice QCD, the expectation value of disconnected quark loops can be written as [11]

$$\left\langle\bar{\psi}\Gamma\psi\right\rangle = -\mathrm{Tr}\left(\Gamma M^{-1}\right), \tag{1}$$

where $\Gamma\in\left\{\mathbb{1},\gamma_\mu,\gamma_5,\gamma_5\gamma_\mu,\sigma_{\mu\nu},\mu,\nu=1,2,3,4\right\}$, and M is the Dirac fermion operator. In this work, we use Wilson's Dirac operator, which can be written as

$$M=\mathbb{1}-\kappa D,\quad \kappa=\frac{1}{2(am+4)}, \tag{2}$$

$$D(n|m)_{\substack{\alpha\beta\\ ab}}=\sum_{\mu=1}^{4}\left(1-\gamma_\mu\right)_{\alpha\beta}U_\mu(n)_{ab}\delta_{n+\hat{\mu},m} +\sum_{\mu=1}^{4}\left(1+\gamma_\mu\right)_{\alpha\beta}U_{-\mu}(n)_{ab}\delta_{n-\hat{\mu},m}, \tag{3}$$

where a is the lattice spacing, and D is referred to as the hopping matrix. The real number κ is the hopping parameter [12]. To calculate the disconnected diagrams, we need to solve the equation

$$Mx=b, \tag{4}$$

where M is the Dirac matrix with dimension $K\times K$, and b is the source vector of dimension $K\times 1$. The solution of this equation is

$$x=M^{-1}b. \tag{5}$$

The evaluation of disconnected quark loops requires M^{-1} connecting arbitrary pairs of lattice points. Generally, Wilson's Dirac matrix is a large sparse matrix and its typical dimension K is from 10^6 up to 10^9. Its direct evaluation is prohibitively expensive, both in terms of computer time and memory.

In order to calculate disconnected quark loops, specif-

Received 22 November 2019, Published online 14 February 2020

* Supported by National Natural Science Foundation of China (11335001)

1) E-mail: zjuercz@zju.edu.cn

2) E-mail: jbzhang08@zju.edu.cn

3) E-mail: xionggy@zju.edu.cn

ic techniques must be introduced. Unbiased noise methods are traditionally used to estimate the inverse matrix [13, 14]. The truncated solver method (TSM) [15] and the spin explicit method (SEM) [16, 17] were introduced to reduce the stochastic error. A probing technique is also a way to deal with this problem [18]. However, we found that all stochastic methods result in large errors in the calculations of disconnected quark loops $\mathrm{Tr}\left(\Gamma M^{-1}\right)$. Hence, we introduce the symmetric multi-probing source (SMP) method to calculate all disconnected quark loops, and compare the results with the $Z(2)$ noise and spin-color explicit (SCE) methods. All comparisons are based on the point source results which are taken as exact.

2 Methods

2.1 $Z(2)$ noise method

In general, the inverse of a large sparse matrix can be calculated by using the unbiased stochastic method. Here, we briefly review the $Z(2)$ noise method. We assume L column noise vectors b^1, b^2, b^3,..., b^L, which have the following two properties [13],

$$\langle b_i\rangle = \frac{1}{L}\sum_{l=1}^{L} b_i^l = O\left(1/\sqrt{L}\right), \tag{6}$$

$$\left\langle b_i b_j\right\rangle = \frac{1}{L}\sum_{l=1}^{L} b_i^l b_j^l = \delta_{ij} + O\left(1/\sqrt{L}\right), \tag{7}$$

where b_i^l is the i-th entry in the noise vector l. The stochastic average $<\cdots>$ is taken over the ensemble of noise vectors L.

If $Z(2)$ noise vectors are used in Eq. (4), we obtain

$$x_i^l = \sum_k M_{ik}^{-1} b_k^l. \tag{8}$$

The inverse matrix element, M_{ij}^{-1}, is given as

$$< b_j x_i >= \sum_k M_{ik}^{-1} < b_j b_k >= M_{ij}^{-1}. \tag{9}$$

The variance of the $Z(2)$ noise method is [19]

$$\sigma^2 \equiv \frac{1}{L}\sum_{i\neq j}^{K}\left|M_{ij}^{-1}\right|^2. \tag{10}$$

It can be seen that the stochastic error of the $Z(2)$ noise estimate results only from the off-diagonal elements of the inverse matrix.

Therefore, we obtain $\mathrm{Tr}(\Gamma M^{-1})$

$$\begin{aligned}\mathrm{Tr}\left(\Gamma M^{-1}\right) &= \sum_j \Gamma M_{jj}^{-1} = \sum_{i,j}\Gamma M_{ij}^{-1}\delta_{ij}\\ &= \sum_{i,j}\frac{1}{L}\sum_l \Gamma M_{ij}^{-1} b_i^l b_j^l = \sum_i \frac{1}{L}\sum_l b_i^l\left(\Gamma x_i^l\right).\end{aligned} \tag{11}$$

In order to reduce the error of the $Z(2)$ noise method, we applied an independent stochastic inversion of the spin and color components (spin-color explicit method, SCE method) for each $Z(2)$ noise vector, similar to SEM [16].

2.2 SMP method

The SMP source vector ϕ_P is introduced as follows [20]

$$\phi_P(S(x,P),\alpha,a) = \sum_{y\in S(x,P)} \psi(y,\alpha,a), \tag{12}$$

where α is the Dirac index and a the color index. $S(x,P)$ represents the sites with the same color of x obtained by the symmetric coloring scheme $P\left(\frac{n_s}{d},\frac{n_s}{d},\frac{n_s}{d},\frac{n_t}{d},mode\right)$, where n_s and n_t are the spatial and temporal sizes of the lattice. d is the distance parameter, and $mode = 0,1,2$ corresponds to the Normal, Split and Combined mode. x is the seed site at (x_1,x_2,x_3,x_4) and y are the other lattice sites belonging to the set $S(x,P)$. ψ is the normalized point source vector. The number of SMP sources $N_{\rm SMP}$ that cover all lattice sites is

$$N_{\rm SMP} = \begin{cases} 12d^4 & mode = 0,\\ 24d^4 & mode = 1,\\ 6d^4 & mode = 2.\end{cases} \tag{13}$$

Applying the SMP source in Eq. (4) to calculate the trace of ΓM^{-1}, we obtain

$$\begin{aligned}\mathrm{Tr}\left(\Gamma M^{-1}\right)_{\rm SMP} &= \sum_{x,\alpha,a}\psi(x,\alpha,a)\left(\Gamma M^{-1}\right)\phi_P(S(x,P),\alpha,a)\\ &= \sum_{x,\alpha,a}\psi(x,\alpha,a)\left(\Gamma M^{-1}\right)\psi(x,\alpha,a) + \sum_{y\in S(x,P)}^{y\neq x}\sum_{\alpha,a}\psi(x,\alpha,a)\left(\Gamma M^{-1}\right)\psi(y,\alpha,a)\\ &= \mathrm{Tr}\left(\Gamma M^{-1}\right) + \sum_{y\in S(x,P)}^{y\neq x}\sum_{\alpha,a}\psi(x,\alpha,a)\left(\Gamma M^{-1}\right)\psi(y,\alpha,a),\end{aligned} \tag{14}$$

where the second term in the last line is the sum of off-diagonal elements of ΓM^{-1}. Considering the space-time locality of M, this term can be regarded as the error in the calculation of $\mathrm{Tr}\left(\Gamma M^{-1}\right)$. If we choose the proper scheme P of the SMP source, the error is quite small. In this case, we can neglect the error term and get

$$\mathrm{Tr}\left(\Gamma M^{-1}\right) \approx \mathrm{Tr}\left(\Gamma M^{-1}\right)_{\mathrm{SMP}}. \tag{15}$$

3 Simulation details

It is very time consuming to solve Eq. (4) if b is the point source (p-s) vector which runs over all lattice sites of a large lattice. In this work, we use the point source method to evaluate $\mathrm{Tr}\left(\Gamma M^{-1}\right)$, and take the result as exact, and use it for comparison. We only work with ensembles of Iwasaki pure gauge configurations, where the volume is $L_\sigma^3 \times L_\tau = 12^3 \times 24$. The lattice spacing of the ensembles is $a \approx 0.1$ fm. The analysis is performed on 25 configurations with $\kappa = 0.151$, corresponding to $m_\pi \approx 488$ MeV. We show the results for $\mathrm{Tr}\left(M^{-1}\right)$ and $\mathrm{Tr}\left(\gamma_5 M^{-1}\right)$ in the main body of this paper. The results for $\mathrm{Tr}\left(\gamma_3 M^{-1}\right)$, $\mathrm{Tr}\left(\gamma_5\gamma_1 M^{-1}\right)$ and $\mathrm{Tr}\left(\sigma_{34} M^{-1}\right)$, selected as representative, are presented in appendix A.

Using the identity $M = \gamma_5 M^\dagger \gamma_5$ [21], we obtain

$$\begin{aligned}\mathrm{Tr}\left(\gamma_5 M^{-1}\right) &= \mathrm{Tr}\left(\gamma_5\gamma_5\left(M^{-1}\right)^\dagger \gamma_5\right)\\ &= \mathrm{Tr}\left(\left(M^{-1}\right)^\dagger \gamma_5\right) = \mathrm{Tr}\left(\left(\gamma_5 M^{-1}\right)^\dagger\right).\end{aligned} \tag{16}$$

Therefore, $\mathrm{Tr}\left(\gamma_5 M^{-1}\right)$ is a real number, and $\mathrm{Tr}\left(M^{-1}\right)$ is also real. The absolute error Δr discussed in this work is defined as

$$\Delta r = \left|r_p - r_m\right|, \tag{17}$$

where r_p is the result for the point source and r_m is the result for any other method.

We also define the method error σ as

$$\sigma^2 = \frac{1}{N_{\mathrm{conf}}(N_{\mathrm{conf}}-1)} \sum_{i=1}^{N_{\mathrm{conf}}} \Delta r_i^2. \tag{18}$$

Δr_i is the absolute error of the i-th configuration (conf), and N_{conf} is the number of configurations. In the definition of σ, we use r_p and not the average value $\langle r \rangle_c$ of all configurations, to eliminate the fluctuations due to different configurations. Therefore, this definition gives only the error of the method.

4 Results and analyses

The results and absolute errors of the first ten configurations are shown as representative in this paper. However, we show the method error for all 25 configurations. For the SMP method, the results for $\mathrm{Tr}\left(M^{-1}\right)$ are shown in Table 1, and in Table 2 for $\mathrm{Tr}\left(\gamma_5 M^{-1}\right)$. The number of source vectors for all methods is the same.

In Figs. 1, 2 and 3, the absolute errors of $\mathrm{Tr}\left(M^{-1}\right)$ for the SMP, $Z(2)$ noise and SCE methods are shown. As expected, as the number of source vectors increases, the absolute errors become smaller for all three methods.

In Fig. 4, $\langle \Delta r \rangle$ of $\mathrm{Tr}\left(M^{-1}\right)$ for the SMP and SCE methods are compared with the $Z(2)$ noise method for the same number of source vectors, indicating that when the number of source vectors is small, the absolute errors of SMP and SCE are larger than of $Z(2)$. The figure also shows that the SCE method does not bring any improvement in the evaluation of the scalar disconnected quark loops compared with the $Z(2)$ noise method. Hence, the $Z(2)$ noise method is an efficient method for the calculation of $\mathrm{Tr}\left(M^{-1}\right)$.

As the number of source vectors increases, the results of the SMP, SCE and $Z(2)$ noise methods become more and more accurate. The results for $\mathrm{Tr}\left(M^{-1}\right)$ show that the $Z(2)$ noise method is a good choice for evaluating the scalar disconnected loops.

The results for $\mathrm{Tr}\left(\gamma_5 M^{-1}\right)$ for the SMP method are

Table 1. Results for $\mathrm{Tr}\left(M^{-1}\right)$ for the SMP method. N is the number of SMP source vectors. The numbers in the parentheses represent the parameters d and *mode* of the SMP source; for example, (6,0) denotes $d = 6$ and *mode* = 0. The SMP method is a good approximation when the number of source vectors is large.

conf.	p-s	N = 15552 (6,0)	N = 3072 (4,0)	N = 1536 (4,2)	N = 384 (2,1)	N = 192 (2,0)	N = 96 (2,2)
1	453821.05	453821.93	453834.19	453831.06	453821.88	453785.60	453890.51
2	454042.56	454049.54	454036.58	454040.99	454020.87	453919.91	453945.70
3	454216.18	454218.24	454219.28	454218.60	454223.99	454389.67	454395.52
4	454002.41	453999.82	453998.76	453994.74	453964.91	454033.19	454069.26
5	454354.48	454357.04	454337.75	454319.32	454291.41	454229.23	454220.83
6	454301.64	454299.51	454308.33	454298.46	454274.90	454210.82	454231.96
7	454085.53	454087.16	454089.11	454085.17	454083.09	454065.35	454038.91
8	454059.63	454060.60	454054.26	454053.96	454016.87	454104.69	454054.37
9	453944.56	453941.69	453936.50	453930.76	453919.66	453778.34	453765.85
10	453914.30	453915.53	453924.14	453923.83	453936.33	453826.90	453825.25

Table 2. Results for $\mathrm{Tr}(\gamma_5 M^{-1})$ for the SMP method. N is the number of SMP source vectors. The numbers in the parentheses represent the parameters d and *mode* of the SMP source.

conf.	*p-s*	N = 15552 (6,0)	N = 3072 (4,0)	N = 1536 (4,2)	N = 384 (2,1)	N = 192 (2,0)	N = 96 (2,2)
1	−18.94	−18.37	−22.18	−15.61	−10.08	−21.66	−22.73
2	202.86	203.21	202.90	212.26	192.83	184.64	188.23
3	183.32	184.33	181.43	180.09	178.41	178.20	148.52
4	−170.65	−170.89	−163.42	−160.16	−186.75	−172.39	−206.26
5	−586.77	−583.80	−563.81	−555.51	−559.26	−569.70	−519.76
6	74.85	73.18	73.35	75.99	81.00	96.71	124.26
7	−288.10	−290.81	−288.23	−284.46	−291.66	−280.63	−271.28
8	141.12	141.86	137.16	138.44	153.09	167.57	164.22
9	−338.58	−335.66	−342.16	−329.44	−338.10	−332.02	−351.82
10	−223.22	−220.96	−224.15	−221.93	−237.32	−218.63	−222.10

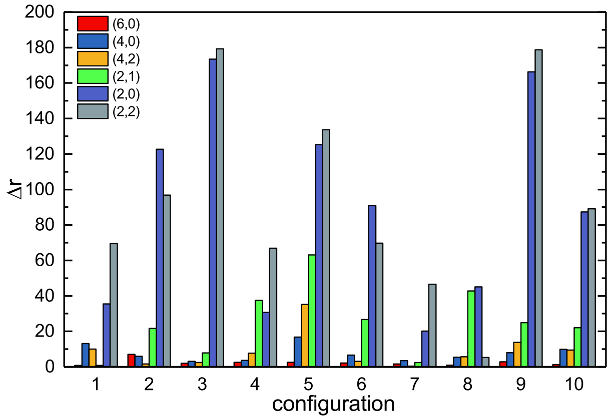

Fig. 1. (color online) Absolute error of $\mathrm{Tr}(M^{-1})$ for the SMP method. The numbers in the parentheses represent the parameters d and *mode* of the SMP source vectors; for example, (6,0) denotes $d=6$ and $mode=0$.

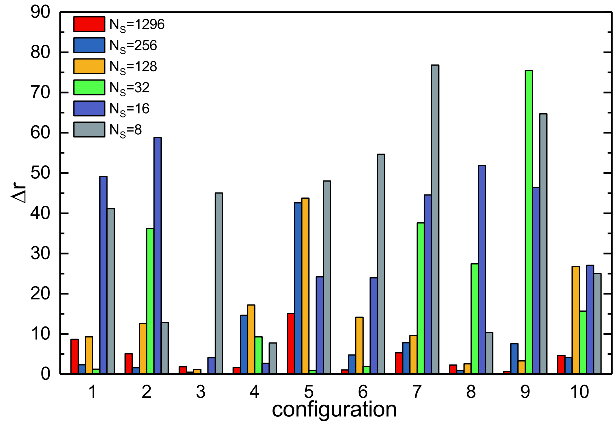

Fig. 3. (color online) Absolute error of $\mathrm{Tr}(M^{-1})$ for the SCE method. N_S is the number of SCE source vectors.

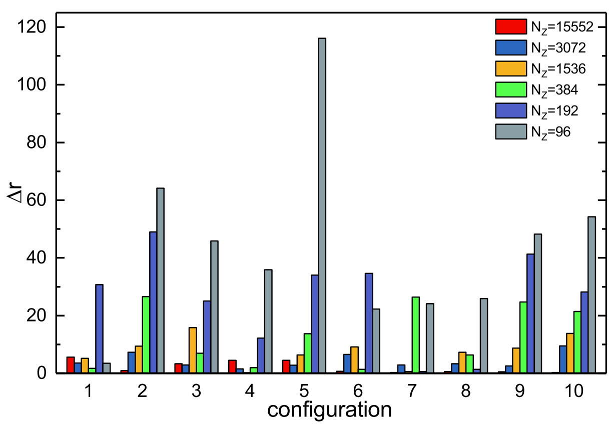

Fig. 2. (color online) Absolute error of $\mathrm{Tr}(M^{-1})$ for the $Z(2)$ noise method. N_Z is the number of $Z(2)$ source vectors.

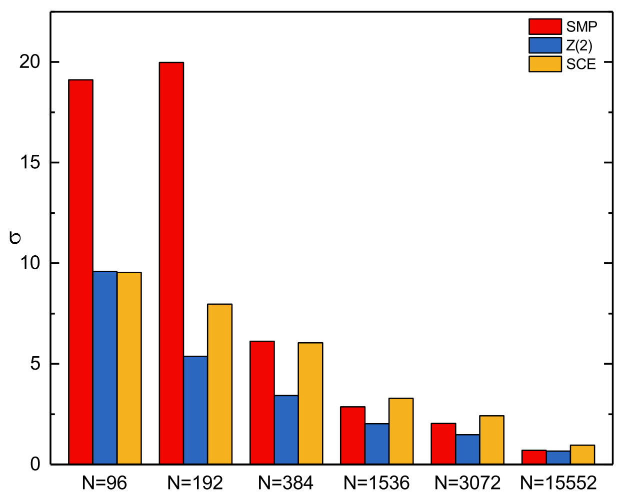

Fig. 4. (color online) σ of $\mathrm{Tr}(M^{-1})$ as a function of the number of source vectors N for the three different methods.

shown in Table 2. The absolute errors of $\mathrm{Tr}\left(\gamma_5 M^{-1}\right)$ are presented in Figs. 5, 6 and 7. As the number of source vectors increases, the absolute errors of all methods decrease, as expected. Fig. 6 shows that the $Z(2)$ noise method gives a too large error of $\mathrm{Tr}\left(\gamma_5 M^{-1}\right)$, especially for small N.

In Fig. 8, the method error of $\mathrm{Tr}\left(\gamma_5 M^{-1}\right)$ is shown, indicating that σ decreases with increasing number of source vectors for all three methods. The SCE method results in a smaller σ than the $Z(2)$ noise method for the same number of source vectors. Hence, the SCE method is an obvious improvement compared with the $Z(2)$ noise method. Also, the SMP method gives a much smaller method error than the $Z(2)$ noise method, especially for a small number of source vectors.

All these results indicate that the $Z(2)$ noise method gives a larger error than the SMP and SCE methods for the same number of source vectors in the calculation of $\mathrm{Tr}\left(\gamma_5 M^{-1}\right)$. Compared with the $Z(2)$ method, the SCE method indeed improves the calculation of $\mathrm{Tr}\left(\gamma_5 M^{-1}\right)$. On the other hand, the absolute errors of the SMP method are smaller than the SCE method. The results of the SMP method are quite precise when the parameter d is large enough. Hence, the SMP method has a considerable advantage over the SCE and $Z(2)$ noise methods in the estimation of $\mathrm{Tr}\left(\gamma_5 M^{-1}\right)$.

In Table 3, $\sigma/\sigma_{Z(2)}$ of the SMP and SCE methods for different N are presented. In the case $\Gamma = 1$, the $Z(2)$ method is the best of the three methods, while for $\Gamma = \gamma_5$, the SMP method gives better results than the others. σ for the SMP method is 22.15% ~ 38.31% of the $Z(2)$ noise method, and about half of the SCE method. Therefore, the SMP method is a considerable improvement in the estimation of pseudoscalar disconnected loops.

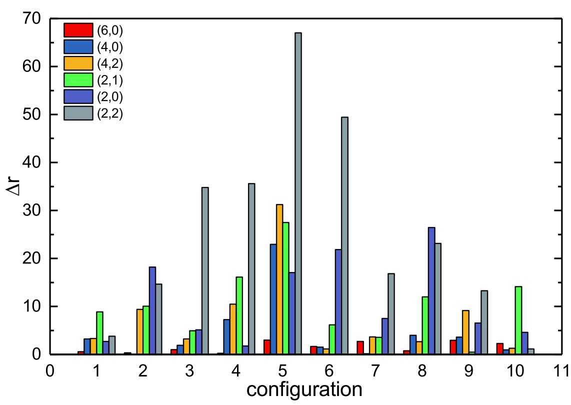

Fig. 5. (color online) Absolute error of $\mathrm{Tr}\left(\gamma_5 M^{-1}\right)$ for the SMP method.

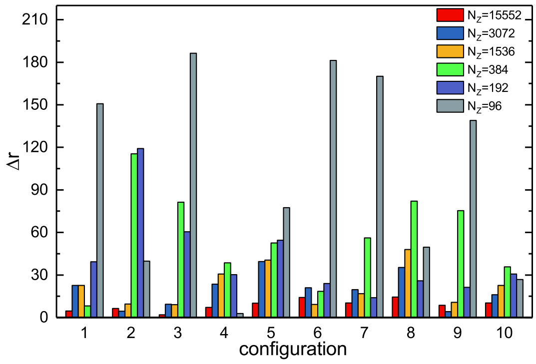

Fig. 6. (color online) Absolute error of $\mathrm{Tr}\left(\gamma_5 M^{-1}\right)$ for the $Z(2)$ noise method.

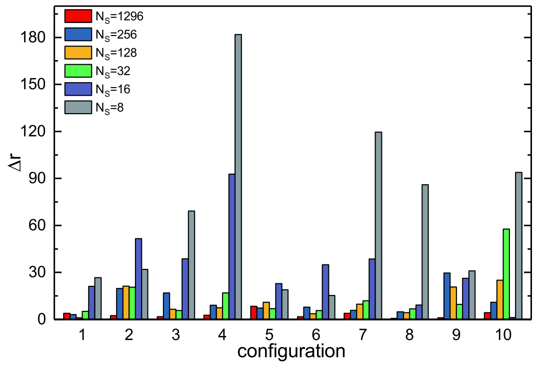

Fig. 7. (color online) Absolute error of $\mathrm{Tr}\left(\gamma_5 M^{-1}\right)$ for the SCE method.

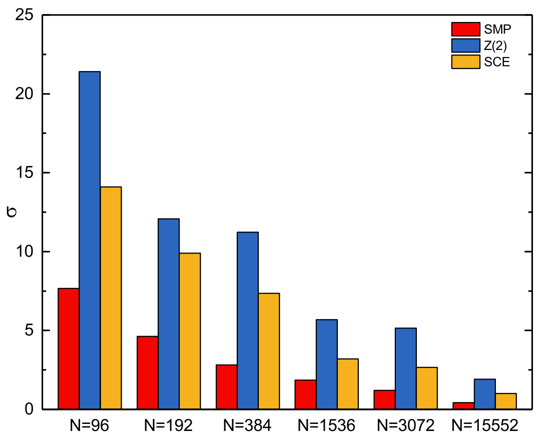

Fig. 8. (color online) Method error of $\mathrm{Tr}\left(\gamma_5 M^{-1}\right)$ as a function of the number of source vectors N.

5 Conclusions

We have calculated in this work all disconnected quark loops using the SMP, SCE and $Z(2)$ noise methods, and presented in the paper a detailed analysis of the results for the scalar and pseudoscalar disconnected quark loops. As expected, the absolute errors of the SMP, SCE and $Z(2)$ noise methods decrease as the number of source vectors in the evaluation of the disconnected quark loops

Table 3. $\sigma/\sigma_{Z(2)}$ for the SMP and SCE methods for different N.

Γ	method	$N = 96$	$N = 192$	$N = 384$	$N = 1536$	$N = 3072$	$N = 15552$
$\mathbb{1}$	SMP	199.22%	371.77%	179.12%	141.37%	138.09%	105.91%
	SCE	99.56%	148.38%	176.85%	161.88%	164.25%	143.99%
γ_5	SMP	35.77%	38.31%	25.13%	32.53%	23.36%	22.15%
	SCE	65.87%	81.97%	65.56%	56.26%	51.62%	52.64%

increases. In the case of scalar disconnected loops, it was shown that the SCE method does not have an advantage over the $Z(2)$ noise method. The absolute errors of the $Z(2)$ noise method are smaller than of the SMP and SCE methods even if the number of source vectors in the calculation of scalar disconnected diagrams is small.

We also found that the SMP method can improve the precision of the calculation of $\mathrm{Tr}\left(\gamma_5 M^{-1}\right)$ by about a factor of 2.5-4.6 compared to the $Z(2)$ noise method, and that the SCE method does not have an advantage over the SMP method. The results show that of the three methods, SMP is the best for the calculation of $\mathrm{Tr}\left(\gamma_5 M^{-1}\right)$. We believe that the SMP method is suitable due to the operator hermiticity, but the reason why it gives a significant improvement in the calculation of pseudoscalar disconnected quark loops requires further study.

Numerical simulations have been performed on the Tianhe-2 supercomputer at the National Supercomputer Centre in Guangzhou (NSCC-GZ), China.

Appendix A: $<\Delta r>$ of the other disconnected quark loops

In this appendix, we show $<\Delta r>$ in Figs. A1, A2, A3 and $\sigma/\sigma_{Z(2)}$ in Table A1 of $\mathrm{Tr}\left(\gamma_3 M^{-1}\right)$, $\mathrm{Tr}\left(\gamma_5\gamma_1 M^{-1}\right)$ and $\mathrm{Tr}\left(\sigma_{34} M^{-1}\right)$, which indicate that the SMP method does not have a significant advantage compared with the $Z(2)$ noise and SCE methods. As the number of source vectors increases, the absolute errors of all methods decrease. When the number of source vectors is large enough, all methods give quite similar results.

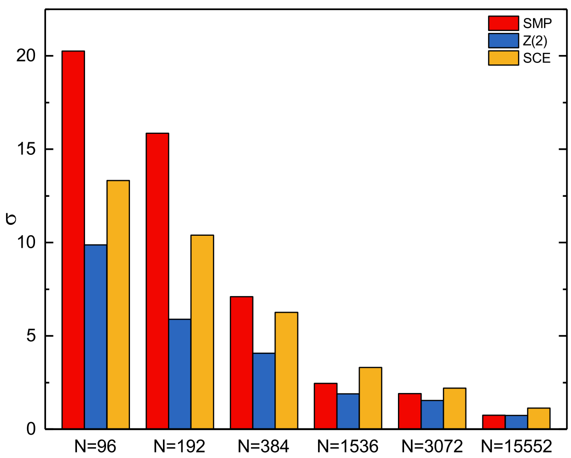

Fig. A1. (color online) σ of $\mathrm{Tr}\left(\gamma_3 M^{-1}\right)$ as a function of the number of source vectors N.

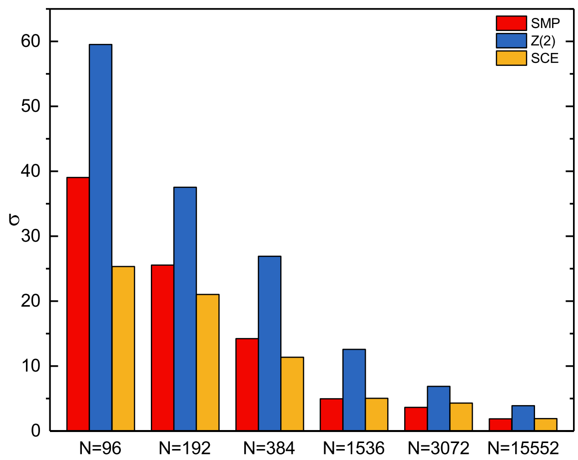

Fig. A2. (color online) Method error of $\mathrm{Tr}\left(\gamma_5\gamma_1 M^{-1}\right)$ as a function of the number of source vectors N.

Table A1. $\sigma/\sigma_{Z(2)}$ for the SMP and SCE methods for different N.

Γ	method	$N = 96$	$N = 192$	$N = 384$	$N = 1536$	$N = 3072$	$N = 15552$
γ_3	SMP	205.18%	269.00%	174.39%	129.72%	123.95%	101.65%
	SCE	134.94%	176.29%	153.68%	174.92%	142.95%	154.08%
$\gamma_5\gamma_1$	SMP	66.81%	63.66%	55.92%	37.60%	52.31%	47.30%
	SCE	43.32%	52.49%	46.56%	41.89%	57.33%	48.15%
σ_{34}	SMP	72.78%	54.20%	47.71%	64.61%	70.62%	73.00%
	SCE	84.09%	60.01%	79.27%	87.96%	90.24%	133.93%

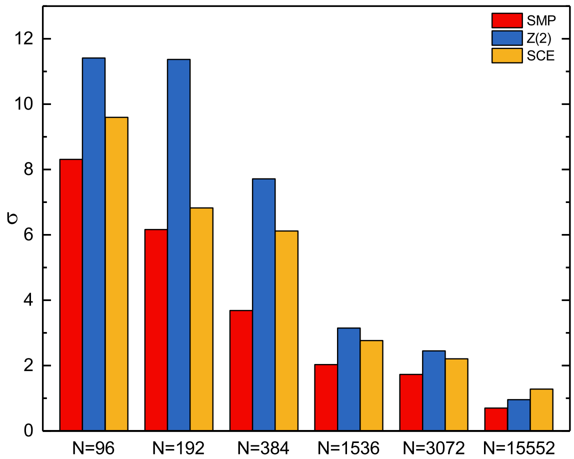

Fig. A3. (color online) Method error of $\mathrm{Tr}\left(\sigma_{34}M^{-1}\right)$ as a function of the number of source vectors N.

References

1 Kenneth G. Wilson, Phys. Rev. D, **10**: 2445-2459 (1974)
2 C. Alexandrou, K. Hadjiyiannakou, G. Koutsou et al, Comput. Phys. Commun., **183**: 1215-1224 (2012)
3 C. Alexandrou, S. Bacchio, M. Constantinou et al, Phys. Rev., **100**(1): 014509 (2019)
4 Shao-Jing Dong and Keh-Fei Liu, Nucl. Phys. Proc. Suppl., **42**: 322-324 (1995)
5 K. Jansen, Christopher Michael, and C. Urbach, Eur. Phys. J. C, **58**: 261-269 (2008)
6 Eric B. Gregory, Alan C. Irving, Chris M. Richards et al, Phys. Rev. D, **77**: 065019 (2008)
7 Randy Lewis, W. Wilcox, and R. M. Woloshyn, Phys. Rev. D, **67**: 013003 (2003)
8 Raza Sabbir Sufian, Yi-Bo Yang, Andrei Alexandru et al, Phys. Rev. Lett., **118**: 042001 (2017)
9 M. Deka, T. Streuer, T. Doi et al, Phys. Rev., **79**: 094502 (2009)
10 B. Chakraborty, C. T. H. Davies, J. Koponen et al, Phys. Rev. D, **98**: 094503 (2018)
11 Suman Baral, Travis Whyte, Walter Wilcox et al, Comput. Phys. Commun., **241**: 64-79 (2019)
12 Christof Gattringer and Christian B. Lang, Lect. Notes Phys., **788**: 1-343 (2010)
13 Shao-Jing Dong and Keh-Fei Liu, Phys. Lett. B, **328**: 130-136 (1994)
14 M. Gong, A. Alexandru, Y. Chen et al, Phys. Rev. D, **88**: 014503 (2013)
15 Gunnar S. Bali, Sara Collins, and Andreas Schafer, Comput. Phys. Commun., **181**: 1570-1583 (2010)
16 J. Viehoff, N. Eicker, S. Gusken et al, Nucl. Phys. Proc. Suppl., **63**: 269-271 (1998)
17 J. Viehoff, Nucl. Phys. Proc. Suppl., **73**: 856-858 (1999)
18 Tang Jok Man and Saad Yousef, HKIE Transactions, **17**(4): 69-72 (2010)
19 C. Thron, S. J. Dong, K. F. Liu et al, Phys. Rev. D, **57**: 1642-1653 (1998)
20 Guang-Yi Xiong, Jian-Bo Zhang, and You-Hao Zou, Chin. Phys. C, **43**(3): 033102 (2019)
21 Walter Wilcox. Noise methods for flavor singlet quantities. In *Numerical challenges in lattice quantum chromodynamics. Proceedings, Joint Interdisciplinary Workshop, Wuppertal, Germany, August 22-24, 1999*, pages 127-141, 1999